MRP8 and MRP14 control microtubule reorganization during transendothelial migration of phagocytes

Thomas Vogl, Stephan Ludwig, Matthias Goebeler, Anke Strey, Irmgard S. Thorey, Rudolf Reichelt, Dirk Foell, Volker Gerke, Marie P. Manitz, Wolfgang Nacken, Sabine Werner, Clemens Sorg, and Johannes Roth

MRP14 (S100A9) is the major calcium-binding protein of neutrophils and monocytes. Targeted gene disruption reveals an essential role of this S100 protein for transendothelial migration of phagocytes. The underlying molecular mechanism comprises major alterations of cytoskeletal metabolism. MRP14, in complex with its binding partner MRP8 (S100A8), promotes polymerization of microtubules. MRP14 is specifically phosphorylated by p38 mitogen-activated protein kinase (MAPK). This phosphorylation inhibits MRP8/MRP14-induced tubulin polymerization. Phosphorylation of MRP14 is antagonistically regulated by binding of MRP8 and calcium. The biologic relevance of these findings is confirmed by the fact that MAPK p38 fails to stimulate migration of MRP14$^{-/-}$ granulocytes in vitro and MRP14$^{-/-}$ mice show a diminished recruitment of granulocytes into the granulation tissue during wound healing in vivo. MRP14$^{-/-}$ granulocytes contain significantly less polymerized tubulin, which subsequently results in minor activation of Rac1 and Cdc42 after stimulation of p38 MAPK. Thus, the complex of MRP8/MRP14 is the first characterized molecular target integrating MAPK- and calcium-dependent signals during migration of phagocytes. (Blood. 2004; 104:4260-4268)

Introduction

Although the initial steps of leukocyte adhesion to endothelial cells during inflammatory reactions have been well characterized in recent years, mechanisms of transmigration remain far less well understood.[1,2] During transendothelial migration leukocytes extensively remodel their cytoskeletal structures in an orchestrated interplay of intracellular signaling pathways involving activation of specific protein kinases and transient elevation of intracellular calcium concentrations.[3-5] Recent reports have focused on the actin filament system and its regulation by the small guanosine triphosphate (GTP)–binding proteins RhoA, Cdc42, and Rac1. Less is known about regulation of the other 2 major cytoskeletal components, intermediate filaments and microtubules (MTs).[6-9] Phagocytes are characterized by a highly dynamic turnover of MTs during transmigration, but the specific proteins that regulate these events have not yet been identified.[10,11] Reorganization of MTs is controlled by modulation of intracellular calcium levels and specific protein phosphorylation.[3,5,12,13] Elevation of intracellular calcium concentrations induces conformational changes of calcium-binding proteins allowing interaction with distinct intracellular targets. The major calcium-binding molecules expressed in neutrophils and monocytes are myeloid-related protein 8 (MRP8 [S100A8]) and MRP14 (S100A9), 2 members of the S100 protein family.[14,15] S100 proteins exhibit functions during various cellular processes such as cell cycle progression and modulation of cytoskeletal-membrane interactions. However, none of the numerous effects of S100 proteins observed in vitro has so far been convincingly confirmed in vivo.[16] Targeted disruption of the *MRP8* gene resulted in a lethal phenotype not allowing further functional analysis.[17] On the other hand, MRP14$^{-/-}$ mice are viable but, at the first glance, do not exhibit an obvious phenotype.[18,19] Calcium-induced complexes of MRP8 and MRP14 colocalize with intermediate filaments and MTs on activation of isolated monocytes.[20-23] Indirect evidence suggests that interaction of MRP8/MRP14 complexes with these cytoskeletal components is modulated by phosphorylation of MRP14 (phospho-MRP14) at Thr113,[23,24] but neither the specific targets within the MT system nor the molecular mechanisms of MRP8/MRP14 action have been identified.

In the present study, we demonstrate that the MRP8/MRP14 complex promotes polymerization of MTs via direct interaction with tubulin. MRP14 acts as a regulatory subunit in the MRP8/MRP14 complex and integrates inputs from 2 major signaling pathways, the p38 mitogen-activated protein kinase (MAPK) cascade and calcium-dependent signal transduction. Targeted gene disruption of MRP14 reveals that MRP8/MRP14 complexes play an essential role during the process of transendothelial migration of phagocytes. The underlying molecular mechanism includes major alterations in tubulin metabolism and in activation pathways of the small GTPases Rac1 and Cdc42.

From the Institute of Experimental Dermatology, Department of Pediatrics, and Institute of Molecular Virology, University of Münster, Germany; Department of Dermatology, University of Würzburg, Germany; Institute of Medical Biochemistry, University of Münster, Germany; Institute of Cell Biology, ETH Zürich, Switzerland; and Institute of Medical Physics and Biophysics, University of Münster, Germany.

Submitted February 5, 2004; accepted July 25, 2004. Prepublished online as *Blood* First Edition Paper, August 26, 2004; DOI 10.1182/blood-2004-02-0446.

Supported by grants from the Interdisciplinary Center of Clinical Research, University of Münster (Fo2/26/04, Na2/009/04; J.R. and W.N.) Deutsche Forschungsgemeinschaft (LU 477/3-3; S.L. and M.G.), and the Bundesministerium für Bildung und Forschung (BMBF; S.W.), Germany.

Reprints: Johannes Roth, Institute of Experimental Dermatology, University of Münster, Röntgenstrasse 21, D-48149 Münster, Germany; e-mail: rothj@uni-muenster.de.

The publication costs of this article were defrayed in part by page charge payment. Therefore, and solely to indicate this fact, this article is hereby marked "advertisement" in accordance with 18 U.S.C. section 1734.

Materials and methods

Cells, cell culture, and mice

Monocytes were isolated from human buffy coats and cultured in McCoy 5a medium supplemented with fetal calf serum (FCS; Gibco Life Technologies, Eggenstein, Germany) in Teflon bags as described earlier.[21] In metabolic labeling experiments, cells were cultivated in macrophage serum-free medium (M-SFM, Gibco Life Technologies) supplemented with granulocyte-macrophage colony-stimulating factor (GM-CSF; Bachem, Braunschweig, Germany). In transendothelial migration assays, purified granulocytes obtained from bone marrow (BM) of MRP14$^{-/-}$ or MRP14$^{+/+}$ mice and endothelial bEND5 cells were used. MRP14$^{-/-}$ mice were generated by targeted gene disruption as described.[19]

Metabolic labeling

Phosphorylation of MRP14 was investigated by metabolic labeling of monocytes with inorganic [^{32}P]-phosphate (Hartmann Analytics, Braunschweig, Germany). Monocytes (3.4×10^6 cells) were incubated in phosphate-free buffer (20 mM HEPES [*N*-2-hydroxyethylpiperazine-*N*′-2-ethanesulfonic acid], pH 7.2, 5.5 mM glucose, 1.8 mM $CaCl_2$, 5.4 mM KCl, 137 mM NaCl, 1% (wt/vol) bovine serum albumin [BSA]) for 45 minutes and, thereafter, for 90 minutes with 20 μCi (0.74 MBq) [^{32}P]-phosphate and stimulated as described. Phosphate incorporation into proteins was detected by phosphorimaging (Fuji BAS 1000, Fuji, via Raytest, Straubenhardt, Germany) and autoradiography after separation of proteins by sodium dodecyl sulfate–polyacrylamide gel electrophoresis (SDS-PAGE; 8%-18%) and blotting onto polyvinylidene difluoride (PVDF) membranes. Specific phosphorylation of MRP14 and equal loading of proteins was ascertained by Western blotting and immunoprecipitation using affinity-purified rabbit antisera monospecific for MRP8 (anti-MRP8) or MRP14 (anti-MRP14) or a monoclonal antibody (mAb; MAC387; Dako, Glostrup, Denmark) against MRP14 as described earlier.[20,21]

Immunoprecipitation and immune complex kinase assays

Monocytes (1×10^7 cells) were stimulated as indicated and lysed in Triton lysis buffer (TLB: 20 mM Tris [tris(hydroxymethyl)aminomethane]–HCl, pH 7.4, 137 mM NaCl, 10% glycerol, 1% Triton X-100, 2 mM EDTA [ethylenediaminetetraacetic acid, 50 mM sodium β-glycerophosphate, 20 mM sodium pyrophosphate, 1 mM Pefablock [Merck, Darmstadt, Germany], 5 μg/mL aprotinin, 5 μg/mL leupeptin, 5 mM benzamidine, and 1 mM sodium orthovanadate) at 4°C for 30 minutes. Cell debris was removed by centrifugation and supernatants were incubated with a polyclonal antiserum against the p38 targets MAPK-activated protein (MAPKAP) kinases 2 and 3 for 2 hours at 4°C. Subsequently, immune complexes were precipitated with protein A-agarose (Roche Molecular Biochemicals, Mannheim, Germany) and washed, first in modified TLB buffer supplemented with 500 mM NaCl and then in kinase buffer (25 mM HEPES, pH 7.5, 10 mM $MgCl_2$, 25 mM sodium-β-glycerophosphate, supplemented with 5 mM benzamindine, 0.5 mM dithiothreitol [DTT], and 1 mM sodium orthovanadate). Samples were then incubated with heat shock protein 27 (Hsp27) as a substrate for MAPKAP kinases 2 and 3 (MAPKAP-K2/3) in the presence of 100 μM unlabeled adenosine triphosphate (ATP), 5 μCi (0.185 MBq) γ-^{32}P]-ATP (Hartmann Analytics), and kinase buffer for 15 minutes at 30°C. Thereafter, samples were boiled in 5 × Laemmli SDS sample buffer and then subjected to SDS-PAGE, blotted onto PVDF membranes, and visualized by autoradiography. Phosphorylated substrates were detected by phosphorimaging. Western blot analysis with a polyclonal antiserum against MAPKAP-K2/3 and an mAb (MAC387) against MRP14 was performed to confirm equal loading of proteins. Every experiment was repeated at least 3 times.

In other sets of experiments, purified MRP14, either nonphosphorylated or in vivo phosphorylated, was incubated with preactivated recombinant p38 in the absence or presence of increasing concentrations of MRP8 or calcium or both. Similar experiments were performed using 3pK (K > M) instead of MRP14 as substrate for p38. MRP8/MRP14 as well as MRP8/phospho-MRP14 complexes were purified as described earlier.[25,26] The monomers MRP8, MRP14, and phospho-MRP14 were isolated by denaturation and dissociation of complexes by addition of 8 M urea and separation of individual subunits by anion-exchange chromatography. Identity of proteins was ascertained by amino acid sequencing and electrospray ionization mass spectrometry. No contamination of MRP14 or MRP8/MRP14 fractions by phospho-MRP14 or vice versa was detectable by mass spectrometry.[25] To confirm the phosphorylation of MRP14 by p38 at Thr113 this amino acid was changed to alanine by site-directed mutagenesis (MRP14-Thr113A1a). Construction of the MRP14 point mutant was performed with the QuickChange Site-directed Mutagenesis Kit (Stratagene, Heidelberg, Germany) according to the manufacturer's instructions using wild-type MRP14 cDNA as template. Recombinant MRP14-Thr113Ala was expressed and purified according to Hunter and Chazin.[27]

Fluorescence measurements

Fluorescence spectra were recorded at 20°C with a spectrofluorometer (Spex FluoroMax II, Instruments SA, Munich, Germany) using protein concentrations of 5 μg/mL in 20 mM Tris-HCl, pH 7.5, including 1 mM DTT. The excitation wavelength was 280 nm (bandpass 1 nm) and the emission scans were recorded between 300 and 400 nm (bandpass 4 nm, integration time 0.5 seconds). Both MRP8/MRP14 and MRP8/phospho-MRP14 complexes were titrated in the presence of calcium concentrations ranging from 0 to 100 μM. The change of the fluorescence emission maximum was plotted as a function of the calcium concentration.

MT spin-down binding assay

Tubulin (final concentration 1.4 mg/mL; Cytoskeleton, Denver, CO) was preassembled for 60 minutes at 37°C to MTs under tubulin-polymerizing conditions (tubulin polymerization buffer (TPB): 20 mM MES/K^+, 5 mM $MgCl_2$, 100 mM glutamate, 3.4 M glycerol, 1 mM GTP, pH 6.8) and subsequently stabilized by 200 μM taxol (Sigma, Deisenhofen, Germany). Binding to MTs was investigated by addition of MRP8/MRP14 or MRP8/phospho-MRP14 complexes or single monomers (molar ratio 1:1 [tubulin heterodimer to MRP heterodimer or MRP monomer, respectively]) in the absence or presence of 60 μM calcium. After incubation for 30 minutes at 37°C samples were loaded onto a cushion buffer (TPB containing a final concentration of 4.35 M glycerol) and centrifuged at 100 000*g*. Pellets and supernatants were analyzed by SDS-PAGE following Coomassie staining.

Tubulin polymerization kinetics

The kinetics of MT polymerization were measured by monitoring changes in optical density at 340 nm as described earlier.[28,29] Samples with a final tubulin concentration of 1.0 mg/mL in TPB were placed in a modified precooled Gilford cell holder at 1°C. Tubulin was mixed either with MRP8/MRP14 complexes or with MRP8/phospho-MRP14 complexes or with the monomers in the presence of either 60 μM calcium (molar ratio of tubulin dimer to MRP8/MRP14 = 10:1) or 0.5 mM EDTA (molar ratio of tubulin dimer toMRP8/MRP14 = 1:1). Polymerization of tubulin was induced by increasing the temperature from 1°C to 37°C.

Transmission electron microscopy and immunogold labeling

MTs were allowed to assemble as described either in the presence or absence of MRP8/MRP14 complexes or calcium or both, then fixed in 1.25% glutaraldehyde. Subsequently, a small droplet of each sample was negatively stained with an aqueous solution of 1% uranyl acetate. For immunogold labeling, samples were first fixed in 1.25% glutaraldehyde and then placed on carbon film–coated nickel grids. Immunolabeling was performed using anti-MRP8 or anti-MRP14 (3 μg/mL) and goat anti–rabbit IgG gold-conjugated (10 nm) second antibodies. Bright-field electron micrographs were recorded by a Philips (Eindhofen, Netherlands) 400 TEM at 80 kV acceleration voltage using Agfa-Gevaert (Leverkusen, Germany) 23D56 film.

MTs/tubulin in vivo assay

The MT content versus free tubulin content was determined using a MT/tubulin in vivo assay from Cytoskeleton (BK038; Cytoskeleton,

Denver, CO). Briefly, 4×10^6 cells/sample of BM-derived granulocytes of MRP14$^{+/+}$ and MRP14$^{-/-}$ mice were homogenized in MT-stabilization buffer (100 mM piperazine diethanesulfonic acid [PIPES], pH 6.9, 5 mM $MgCl_2$, 1 mM EGTA [ethylene glycol tetraacetic acid], 30% (vol/vol) glycerol, 0.1% Nonidet P40, 0.1% Triton X-100, 0.1% Tween 20, 0.1% β-mercaptoethanol, 0.001% Antifoam, supplemented with 1 μg/mL pepstatin, 1 μg/mL leupeptin, 10 μg/mL benzamidine, 500 μg/mL tosyl arginine methyl ester, 0.1 mM GTP, 1 mM ATP) followed by centrifugation (100 000*g*, 30 minutes) to separate the MTs from free tubulin pool. All steps were done at 37°C. Subsequently, protein concentrations were determined using the advanced protein assay reagent (ADV01) from Cytoskeleton. Equal amounts of protein were separated on SDS-PAGE (8%) and tubulin bands were identified by Western blot using mAb against α-tubulin (ICN, Meckenheim, Germany). Bands were quantified using the software Lumi-Analyst 3.0 of the Lumi-Imager F1 from Boehringer (Mannheim, Germany).

Rac1, Cdc42, and RhoA activation assays

An affinity precipitation or pull-down assay for activated GTPases using GST-tagged PAK-PBD (p21-activated kinase 1–p21-binding domain) for Rac1 (BK035, Cytoskeleton) and Cdc42 (BK034) or GST-tagged Rhotekin-RBD for RhoA (BK036) was performed to determine the activated fractions (affinity precipitation). In parallel, total content of GTPases was determined by Western blots of cell lysates. Equal numbers of resting BM-derived granulocytes were stimulated for various times (1-5 minutes) with 0.5 mM arsenite (Fluka, Seelze, Germany) in Dulbecco modified Eagle medium (DMEM) at 37°C. The reaction was stopped by addition of ice-cold 2 × lysis buffer (RhoA: 50 mM Tris, pH 7.50, 10 mM $MgCl_2$, 0.5 M NaCl, 1% Triton X-100, and protease inhibitor cocktail [PIC]: 10 μg/mL leupeptin, 10 μg/mL aprotinin, 500 μg/mL tosyl arginine methyl ester; Rac1: 50 mM Tris, pH 7.5, 10 mM $MgCl_2$, 0.3 M NaCl, 2% IGEPAL, 10% sucrose, PIC; Cdc42: same as for Rac1 but without 10% sucrose) and the lysate was immediately centrifuged for 5 minutes at 6000*g* at 4°C. After extraction there were no GTPases detectable in the unsoluble fraction in both MRP14$^{-/-}$ and MRP14$^{+/+}$ granulocytes. The supernatants were added to 25 μg PBD-agarose conjugates or to 33 μg RBD-agarose conjugates (Cytoskeleton), rotated for 60 minutes at 4°C, and followed by 2 washes of the protein complexes with 1 × lysis buffer and wash buffer (25 mM Tris, pH 7.5, 30 mM $MgCl_2$, 40 mM NaCl). Bound proteins were dissociated and denatured by heating in sample buffer at 95°C for 5 minutes and subjected to SDS-PAGE (12%) and Western blot using nitrocellulose membranes. Rac1, Cdc42, and RhoA proteins were visualized using antibodies against the individual GTPases (rabbit antisera against RhoA, Rac1, or Cdc42, all from Cytoskeleton) and chemiluminescence techniques.

Wounding and preparation of wound tissues

Mice were anesthetized and 4 full-thickness excisional wounds 5 mm in diameter were generated on the back of 8 wild-type mice and 8 MRP14$^{-/-}$ mice (all female, 9 weeks of age) by excising skin and panniculus carnosus as described.[30,31] Wounds were harvested after 5 days. For histologic analysis, 2 complete wounds per animal were isolated, bisected, fixed overnight in 4% paraformaldehyde in phosphate-buffered saline (PBS; for histology) or in 95% ethanol/1% acetic acid (for immunofluorescence), and embedded in paraffin. Sections (7 μm) were analyzed using hematoxylin-eosin and Masson trichrome staining or immunofluorescence. The extent of wound closure was determined morphometrically on selected sections from the middle of the wound (8 for wild-type and 8 for MRP14$^{-/-}$) and is indicated as the distance between the tips of the 2 epithelial tongues, in percent of the distance between the wound edges (border between dermis and granulation tissue).

Immunofluorescence microscopy

BM-derived murine MRP14$^{+/+}$ and MRP14$^{-/-}$ granulocytes were cultured on fibronectin-coated (Becton Dickinson, Heidelberg, Germany) LabTec chamber slides (Nunc, Wiesbaden, Germany) for 2 hours. Cells were fixed with methanol (−20°C, 4 minutes) and acetone (−20°C, 4 minutes) and processed for single-labeling immunofluorescence as described earlier[20] using mAb against α-tubulin from ICN.

Sections from the middle of 5-day wounds were incubated overnight at 4°C with a rabbit polyclonal antibody directed against keratin 6 (BabCo, Richmond, CA), a mAb directed against keratin 10 (Dako, Hamburg, Germany), and a rat mAb directed against the neutrophil marker Ly-6G (BD Biosciences, Heidelberg, Germany). Incubation with the primary antibodies was followed by a 1-hour incubation at room temperature with cyanine 3 (Cy3)–conjugated anti–rabbit IgG, Cy2-conjugated anti–rat IgG, and Cy5-conjugated anti–mouse IgG (Jackson ImmunoResearch Labs, West Grove, PA). Subsequently, slides were washed in PBS, prior to mounting in Tris/glycerol-containing n-propyl-gallate. Specimens were analyzed using confocal microscopy on an inverted DM IRB/E microscope equipped with a true confocal scanner (TCS SP1) and a PL/APO 63/1.32 oil immersion objective (Leica), as well as argon and helium-neon lasers. Image processing was done on a Silicon Graphics workstation using Imaris (Bitplane, Zurich, Switzerland), a 3-dimensional multichannel image processing software specialized for confocal microscopy data sets. The numbers of Ly-6G$^+$ cells were quantified in MRP14$^{+/+}$ and MRP14$^{-/-}$ mice.

Detection of calcium-binding proteins

Calcium binding of proteins was determined by a calcium overlay assay.[23] Lysates of granulocytes obtained from MRP14$^{-/-}$ or MRP14$^{+/+}$ mice were separated by SDS-PAGE and blotted onto nitrocellulose membranes. Binding of [^{45}Ca]$CaCl_2$ was detected by autoradiography.

Transmigration assay

Transmigration assays were performed using murine endothelial cells (bEND5) that were grown as monolayers for 3 days on fibronectin-coated 5-μm pore size Transwell filters (Costar, Bodenstein, Germany) as described.[32] Murine BM-derived granulocytes of MRP14$^{+/+}$ and MRP14$^{-/-}$ mice were added in the upper chamber and allowed to transmigrate for 4 hours at 37°C. The number of migrated granulocytes was counted in a Coulter Counter Z2 (Coulter, Krefeld, Germany). Experiments were done in quadruplicate. Integrity of endothelial monolayers was verified morphologically and by measuring transendothelial resistance using an EVOMTM-epithelial volt-ohmmeter (World Precision Instruments, Sarasota, FL).[32]

Statistical analysis

Statistically significant differences were calculated by the *U* test according to Mann and Whitney (for values with nonparametric distribution). Values of *P* greater than .05 were considered to be not significant. All results shown are mean plus or minus SEM.

Results

MRP14 is specifically phosphorylated by MAPK p38

Transendothelial migration of phagocytes requires rearrangement of their cytoskeleton. Complexes of MRP8 and MRP14 have been proposed to modulate membrane-cytoskeletal interactions in a calcium-dependent manner involving MRP14 phosphorylation.[21,23,24] We now demonstrate that stimulation of monocytes with arsenite, an activator of the p38 MAPK pathway, led to a strong incorporation of [^{32}P]-phosphate into MRP14 (Figure 1A). Exposure to phorbol myristate acetate (PMA), an activator of extracellular signal-regulated kinases 1 and 2 (ERK1/ERK2) and protein kinase C, had only minor effects, whereas anisomycin, an activator of both JNK/SAPK and p38 MAPK cascades, strongly increased MRP14 phosphorylation as well (Figure 1B). SB202190 (Calbiochem, Bad Soden, Germany), a specific inhibitor of p38, efficiently blocked both arsenite- and anisomycin-induced phosphorylation of MRP14, whereas PD98059 (Calbiochem), an inhibitor of MEK (MAPK kinase), the upstream kinase of ERK, had no such effect (Figure 1A-B). We further observed a significant basal phosphorylation of MRP14, which was blocked by incubation with SB202190 for 30 minutes (Figure 1B). Identical results were obtained using another

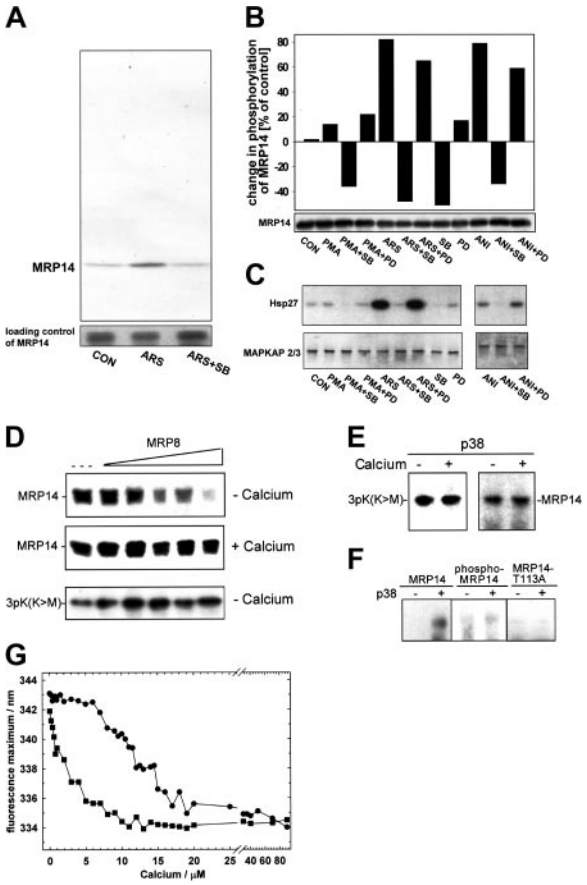

Figure 1. Phosphorylation of MRP14 by p38 MAPK in monocytes. (A) [^{32}P]-Phosphate-labeled monocytes were stimulated with arsenite (ARS, 0.5 mM) for 15 minutes with or without preincubation with pharmacologic p38 inhibitor SB202190 (ARS + SB, 7 μM) for 30 minutes. MRP14 was immunoprecipitated and analyzed by SDS-PAGE and autoradiography (upper panel). All experiments presented in this figure were performed at least 3 times. Equal amounts of immunoprecipitated MRP14 were confirmed by Western blotting using a mAb to MRP14 (lower panel). (B) [^{32}P]-Phosphate-labeled monocytes were incubated with medium as control (CON), 100 nM PMA, 0.5 mM arsenite (ARS), or 5 μg/mL anisomycin (ANI) for 15 minutes as indicated. In some experiments, monocytes were preincubated with SB202190 (SB, 7 μM) or PD98059 (PD, 20 μM) for 30 minutes. Data are shown as percent change of [^{32}P]-phosphate incorporation into MRP14 as compared to nonstimulated cells (CON). Phosphorylation was analyzed by phosphorimaging of MRP14 bands after SDS-PAGE. Protein loads were confirmed by Western blotting using a mAb against MRP14 (lower panel). (C) Monocytes were stimulated as described in panel B. Activation of p38 MAPK was studied indirectly by determining the activity of the downstream kinase MAPKAP-K2/3 using Hsp27 as substrate (upper panel). Protein loads were confirmed by Western blotting using an antiserum to MAPKAPK-2/3 (lower panel). (D) Purified MRP14 (5 μg) was incubated with active recombinant p38 MAPK and 5 μCi (0.185 MBq) γ[^{32}P]-ATP for 15 minutes in the presence of increasing amounts of MRP8 (0-10 μg) in the absence or presence of 60 μM calcium as indicated. When MRP14 was replaced by 3pK (K > M) as substrate, no inhibitory effect of MRP8 was observed. Incorporation of [^{32}P]-phosphate into MRP14 and 3pK (K > M) was visualized by SDS-PAGE and autoradiography. Similar results were obtained when immunoprecipitating preactivated p38 from transfected embryonic kidney 293 cells (data not shown). (E) Purified MRP14 or 3pK (K > M) was incubated with preactivated p38 and 5 μCi (0.185 MBq) γ[^{32}P]-ATP in the absence or presence of 60 μM calcium and studied as described. Addition of calcium had no influence on p38 activity, as indicated by the lack of effects on phosphorylation of MRP14 or 3pk (K > M). (F) MRP14 and phospho-MRP14 were purified from human granulocytes and MRP14-T113A from transfected *E coli* BL21 cells and incubated with preactivated p38 and γ[^{32}P]-ATP and processed as described in panel A. Only the nonphosphorylated isoform of MRP14 shows incorporation of [^{32}P]-phosphate in the presence of preactivated p38. Data shown are representative for at least 3 independent experiments. (G) Purified MRP8/MRP14 (■) and MRP8/phospho-MRP14 (●) were exposed to increasing concentrations of calcium, and conformational changes of the protein complex were detected by changes of the intrinsic fluorescence maximum (protein concentration, 5 μg/mL). Phosphorylation of MRP14 shifted conformational changes to higher calcium concentrations. Data represent means of 4 independent experiments (maximal deviation between individual experiments < 0.7 nm).

p38-specific inhibitor (SB203580, data not shown). Densitometric quantification of basal MRP14 phosphorylation revealed that about 35% of the signals can be attributed to MRP14. This fraction increased further up to 50% after activation of p38. This indicates that MRP14 is the major phosphorylated protein in both nonstimulated and arsenite-activated monocytes. The effects of arsenite and anisomycin on MRP14 phosphorylation in monocytes were perfectly paralleled by changes in p38 activity, as assayed by the activation profile of its downstream kinase MAPKAP-K2/3 (Figure 1C).

We next investigated the mechanism of MRP14 phosphorylation using an in vitro assay. When active recombinant p38 MAPK was incubated with MRP14 in the presence of γ-^{32}P]-ATP, a strong phosphorylation of MRP14 was seen (Figure 1D). Because MRP14 forms complexes with MRP8, we added MRP8 to the MRP14 phosphorylation assay. Surprisingly, increasing concentrations of MRP8 significantly inhibited phosphorylation of MRP14 by p38. This effect was specific for MRP14, because phosphorylation of another p38 substrate, 3pK (K > M), was not influenced by MRP8. However, in the presence of calcium the inhibitory effect of MRP8 on p38-induced MRP14 phosphorylation was completely antagonized (Figure 1D). Calcium itself had no direct effect on the phosphorylation of MRP14 or other p38 substrates (Figure 1E). Our data suggest that calcium was inducing conformational changes in the MRP8/MRP14 complex, which allowed phosphorylation of MRP14 by p38. In contrast to purified nonphosphorylated MRP14, in vivo prephosphorylated MRP14 did not incorporate labeled phosphate on incubation with active p38, confirming the physiologic significance of the phosphorylation site targeted by p38 in vitro. To further confirm the identity of the phosphorylation site we constructed a mutant of MRP14 (MRP14-T113A) where Thr113 was substituted by alanine. Indeed we could not observe phosphorylation of MRP14-T113A, confirming that p38 kinase phosphorylates exclusively Thr113 of MRP14 (Figure 1F).

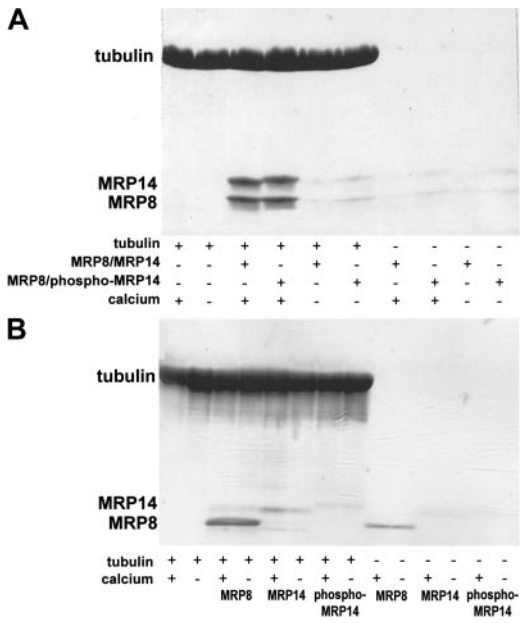

Figure 2. Binding of MRP8 or MRP14 to tubulin. (A) Prepolymerized and Taxol-stabilized MTs were incubated with MRP8/MRP14 or MRP8/phospho-MRP14 complexes at an equimolar ratio (tubulin dimer to MRP8/MRP14 = 1:1) in the absence or presence of 60 μM calcium. Binding to tubulin filaments was then analyzed by spin-down binding assays and Coomassie blue stainings after SDS-PAGE. (B) Binding to tubulin was analyzed as described in panel A using isolated subunits of MRP8, MRP14, or phospho-MRP14. The interaction of MRP8/MRP14 complexes with tubulin was not affected by addition of up to 300 mM NaCl (data not shown). All experiments presented in this figure were performed at least 3 times.

To analyze the effects of MRP14 phosphorylation on the calcium-binding properties of MRP8/MRP14 complexes we determined conformational changes by examination of the fluorescence emission maximum of MRP8/MRP14 and MRP8/phospho-MRP14 in the presence of increasing calcium concentrations. MRP8/MRP14 complexes significantly changed their conformation at a calcium concentration between 0 and 10 μM, as indicated by a blue shift in the emission maximum (Figure 1G). Interestingly, phosphorylation of MRP14 led to a strong shift of the dose-response graph to higher calcium concentrations, indicating that after phosphorylation the induction of conformational changes required significantly higher calcium concentrations.

Complexes of MRP8 and MRP14 promote polymerization of tubulin filaments

MRP8/MRP14 complexes colocalize with MTs on activation of monocytes.[20] We therefore analyzed direct interactions of MRP8 and MRP14 with tubulin in the absence or presence of calcium. Binding was investigated in a spin-down binding assay using prepolymerized and Taxol-stabilized tubulin filaments (Figure 2). MRP8/MRP14 complexes bound to tubulin filaments in a calcium-dependent manner unaffected by phosphorylation of MRP14 (Figure 2A). Individual analysis of the 2 MRP subunits revealed that MRP8 was primarily responsible for the interaction with tubulin filaments (Figure 2B). The K_d of MRP8/MRP14 for binding of tubulin is 0.14 ± 0.05 μM, affirming specificity of this interaction (data not shown).

We then analyzed the functional effects of MRP8 and MRP14 on MT formation using an in vitro polymerization assay. Under conditions that allow spontaneous polymerization of tubulin (37°C, 3.4 M glycerol),[29] we found that addition of nonphosphorylated MRP8/MRP14 complexes significantly accelerated and potentiated polymerization of tubulin (molar ratio of tubulin dimer to MRP8/MRP14 = 1:1). Similar results were observed even with a 10-fold molar excess of tubulin compared to MRP8/MRP14 (data not shown). In contrast, addition of MRP8/phospho-MRP14 only showed minor effects (Figure 3A). With a buffer system containing 1.1 M glycerol no spontaneous polymerization of tubulin was observed,[29] but polymerization of tubulin could be induced on addition of nonphosphorylated MRP8/MRP14 complexes. MRP8/phospho-MRP14 complexes or lower concentrations of MRP8/MRP14 yielded only minor effects (Figure 3B). In contrast to its

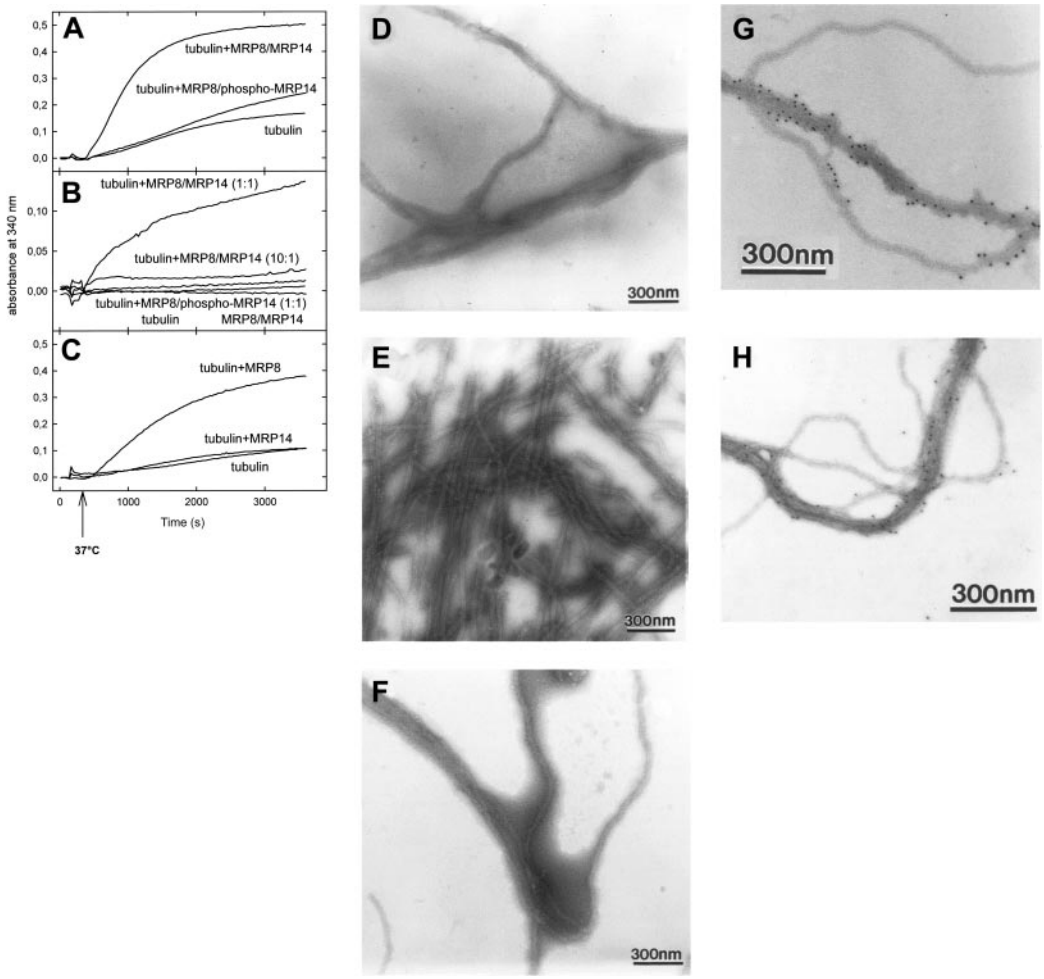

Figure 3. Influence of MRP8 and MRP14 on tubulin polymerization. Tubulin (final concentration 1 mg/mL) was mixed with MRP8/MRP14, MRP8/phospho-MRP14 complexes (A-B), or MRP8 or MRP14 monomers (C) under either polymerizing (3.4 M glycerol in panels A and C, molar ratio of tubulin to MRP = 1:1) or nonpolymerizing conditions (panel B, 1.1 M glycerol, molar ratio of tubulin to MRP as indicated in the figure). Tubulin and MRP8/MRP14 alone were used as controls. Polymerization was induced by elevating the temperature from 1°C to 37°C within 210 seconds, and formation of tubulin filaments was monitored by measuring optical density at 340 nm for at least 1 hour. Each experiment was repeated at least 3 times. (D-H) Transmission electron micrographs of samples prepared as above (ratio of tubulin dimer to MRP8/MRP14 dimer = 10:1, 60 μM calcium). Tubulin filaments polymerized in the absence (D) or presence (E) of MRP8/MRP14; in the presence of MRP8/phospho-MRP14 (F); or in the presence of MRP8/MRP14 with localization of MRP14 by immunogold labeling (G- H). MRP8/MRP14 shows a clear colocalization with MT bundles, whereas single-stranded tubulin filaments are spared. Immunogold labeling with anti-MRP8 revealed identical patterns (data not shown). Bars represent 300 nm.

known inhibitory properties on tubulin polymerization,[33] calcium increased the promoting effect of MRP8/MRP14 on MT formation. This cannot be explained by simply chelating free calcium ions by MRP8/MRP14 because this effect is also observed in the presence of excess calcium (up to 1 mM) and at molar ratios of tubulin dimer to MRP8/MRP14 = 10:1 (data not shown). In accordance with the binding assays, addition of purified MRP8 enhanced tubulin polymerization (Figure 3C), whereas isolated MRP14 as well as other S100 proteins such as S100A1, S100C, or S100P had no significant effect (Figure 3C and data not shown). However, complexes of MRP8/MRP14 were more effective promoters of tubulin polymerization than isolated MRP8 subunits. These observations indicate an important regulatory role of MRP14 in the MRP8/MRP14 complex.

In addition to these functional assays we analyzed morphologic correlates of MRP8/MRP14-promoted MT formation by transmission electron microscopy (TEM). In the presence of MRP8/MRP14 complexes significantly increased numbers of tubulin filaments were observed, and these were more elongated and threadlike as compared to controls. On adding MRP8/phospho-MRP14 complexes, the situation resembled that observed with tubulin alone (Figure 3D-F). Immunogold labeling with anti-MRP14 (Figure 3G-H) or anti-MRP8 (not shown) revealed that complexes of these S100 proteins were exclusively localized at bundles of MTs rather than at single-stranded tubulin filaments indicating a role of MRP8/MRP14 in cross-linking of MTs.

Cytoskeletal alterations in MRP14$^{-/-}$ mice

To investigate the relevance of our in vitro studies we analyzed MRP14$^{-/-}$ mice generated by targeted gene disruption.[19] As expected, granulocytes obtained from MRP14$^{-/-}$ mice completely lack the MRP14 molecule (Figure 4A). MRP8 protein is accumulated at a significantly reduced level (Figure 4A), whereas MRP8 mRNA expression is not altered (data not shown). This may indicate an accelerated catabolism of MRP8 in the absence of MRP14. As demonstrated by $^{45}Ca^{2+}$ overlay, MRP8 and MRP14 are the major calcium-binding EF-hand proteins in wild-type murine granulocytes. In contrast, MRP14$^{-/-}$ granulocytes did not show a calcium-binding band at 14 kDa, the presumed mass of MRP14, and only minor binding by MRP8 (Figure 4A). Up-regulation of other calcium-binding proteins was not observed, indicating that the overall calcium-binding capacity is reduced in granulocytes of MRP14$^{-/-}$ mice.

Because MRP8/MRP14 complexes regulate MT formation, we analyzed whether deletion of the *MRP14* gene has any effect on the expression of tubulin. Comparing the content of tubulin in MRP14$^{+/+}$ and MRP14$^{-/-}$ granulocytes, we found significantly less tubulin in MRP14$^{-/-}$ cells both as polymerized MTs and as free dimers in the cytoplasm (Figure 4B-C). There are no quantitative differences regarding expression of actin between these cells (Figure 4D).

The small GTPases, Rac1, RhoA, and Cdc42, which regulate cellular migration processes, bind to MTs in their inactive state and are activated during remodeling of MTs. Consistent with the low amounts of tubulin, MRP14$^{-/-}$ granulocytes additionally presented with decreased total levels of GTPases Rac1 and Cdc42 in the resting state (Figure 4D). Furthermore, there was an impressive reduction of activation of Rac1 and Cdc42 after stimulation of p38 MAPK by arsenite in MRP14$^{-/-}$ granulocytes. Total levels as well as activation of Rho GTPase were unchanged in MRP14$^{-/-}$ mice (Figure 4 D-E). These data suggest that the regulatory effect of MRP8/MRP14 on tubulin polymerization subsequently modulates other signaling molecules such as GTPases that are involved in actin metabolism and migration events.

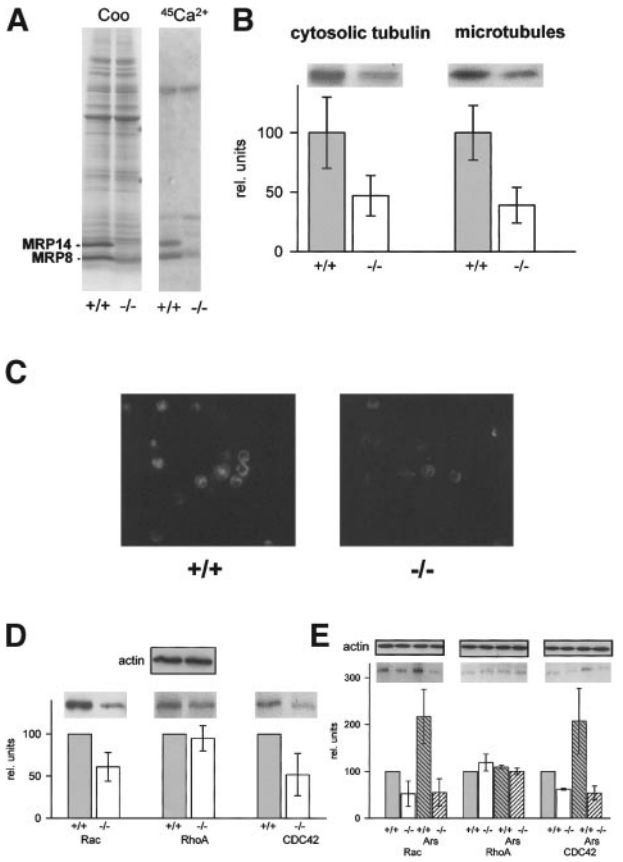

Figure 4. Cytoskeletal alterations in granulocytes of MRP14$^{-/-}$ mice. (A) Lysates of granulocytes obtained from MRP14$^{+/+}$ or MRP14$^{-/-}$ mice were separated by 15% SDS-PAGE and stained by Coomassie blue (Coo) or processed for [^{45}Ca] overlay ($^{45}Ca^{2+}$). In all assays MRP14$^{-/-}$ granulocytes lack MRP14 and present with only a weak band of MRP8. (B) Lysates of granulocytes obtained from MRP14$^{+/+}$ or MRP14$^{-/-}$ mice were separated in microtubule content (right) versus free-tubulin content (left), loaded on an 8% SDS-PAGE, electroblotted on nitrocellulose membrane, and stained with a mAb against α-tubulin. The figure shows representative blots and mean data of 5 independent experiments obtained by densitometric scanning of protein bands. (C) BM-derived granulocytes of MRP14$^{+/+}$ (left) or MRP14$^{-/-}$ mice (right) were cultured for 2 hours on fibronectin-coated LabTec chamber slides. Cells were processed as described in "Materials and methods" and stained with a mAb against α-tubulin. (D) Detergent-soluble proteins from whole-cell lysates of MRP14$^{+/+}$ and MRP14$^{-/-}$ granulocytes were processed for Western blot analysis as described in "Materials and methods," and nitrocellulose membranes were stained with polyclonal antibodies against Rac1, RhoA, or Cdc42, respectively. Data are presented as described in panel B. Using an mAb against actin we confirmed equal protein loads in the common control by Western blotting (upper panel). The figure shows representative blots and mean data of 5 independent experiments obtained by densitometric scanning of protein bands. Controls of individual experiments were set to 100%. (E) Granulocytes of MRP14$^{+/+}$ and MRP14$^{-/-}$ mice were either left untreated or stimulated with 0.5 mM arsenite for 5 minutes at 37°C. Activation was stopped by addition of ice-cold 2 × lysis buffer and lysates were processed for Rac1, RhoA, and Cdc42 activation assays as described. Equal loading of protein was controlled by a mAb against actin (upper panel). Data are presented as described in panel D.

MRP14 plays an important role during migration of phagocytes

To elucidate the physiologic relevance of diminished Rac1 and Cdc42 activation in MRP14$^{-/-}$ granulocytes, we analyzed transendothelial migration in a 2-chamber assay in vitro. Using granulocytes obtained from MRP14$^{+/+}$ mice we observed similar results regarding phosphorylation of murine MRP14 after stimulation of p38 with arsenite as shown (Figure 1) for human monocytes (data not shown). Activation of p38 MAPK by arsenite increased transmigration rates of MRP14$^{+/+}$ granulocytes (4.0 ± 1.2-fold), whereas MRP14$^{-/-}$ cells showed no acceleration of their migratory properties (1.3 ± 0.2-fold; Figure 5A). These data indicate that

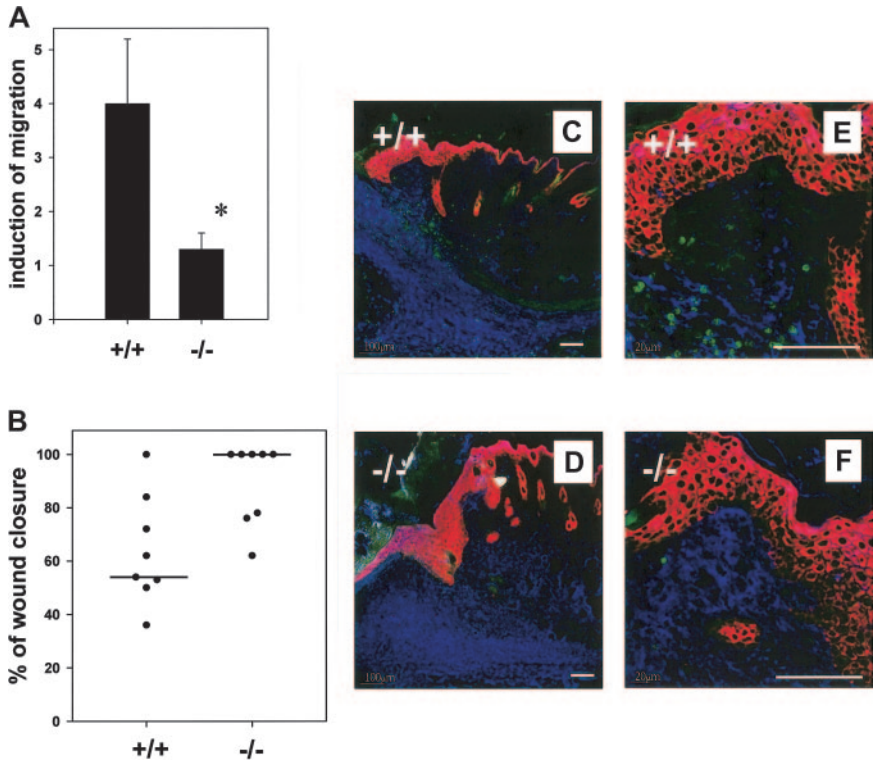

Figure 5. MRP14$^{-/-}$ mice show decreased migration rates of neutrophils during wound healing. (A) Transendothelial migration rates of MRP14$^{+/+}$ and MRP14$^{-/-}$ granulocytes through a monolayer of bEND5 endothelial cells. Granulocytes were either left untreated or preincubated with arsenite for 30 minutes prior to transendothelial migration to activate p38 MAPK. Bars represent n-fold induction of transmigration rates by arsenite stimulation compared to unstimulated control cells of the appropriate mouse strain. * indicates a statistically significant difference ($P \leq .05$). Mean and SD of 5 independent experiments are shown. (B) Mice were wounded as described in "Materials and methods." The extent of wound closure was determined morphometrically on histologic sections prepared from 5-day old wounds of MRP14$^{-/-}$ mice and MRP$^{+/+}$ control littermates (8 wounds each). MRP14$^{-/-}$ mice show a significantly accelerated rate of wound closure as compared to MRP14$^{+/+}$ mice ($P \leq .02$). (C- F) Paraffin sections of 5-day-old murine wounds were stained with antibodies directed against cytokeratin 6 (K6, red), cytokeratin 10 (K10, blue), and the granulocyte-specific antigen Ly6G (green), followed by Cy3-, Cy5-, and Cy2-conjugated secondary antibodies, respectively. Panels C and E present sections of MRP14$^{+/+}$ mice; D and F, sections of MRP14$^{-/-}$ mice at lower (C-D) or higher (E-F) magnifications (bars represent 100 μm). MRP14$^{-/-}$ mice show a significantly lower number of Ly6G^{+} granulocytes in their granulation tissue. Figures shown are representative for 8 animals from each genotype analyzed.

promotion of phagocyte migration by activating the p38 signaling pathway is predominantly mediated by phosphorylation of MRP14.

To determine if the lack of MRP14 also impairs granulocyte migration in vivo, a model of mouse wound healing was applied.[31] We generated full-thickness excisional wounds on the back of MRP14$^{-/-}$ mice and age- and sex-matched wild-type animals. Compared with MRP14$^{+/+}$ mice (660 ± 340 cells/visual field, n = 5), MRP14$^{-/-}$ (170 ± 100 cells/visual field, n = 6) animals showed an about 4-fold reduction of infiltrating granulocytes in 5-day wounds. This indicates that the influx of these cells into skin wounds is impaired in the absence of MRP14 (Figure 5C-F). The lower number of granulocytes in the wound tissue was associated with a significantly accelerated wound closure in MRP14$^{-/-}$ animals compared with MRP14$^{+/+}$ mice (Figure 5B).

Discussion

The family of S100 proteins is the largest group of calcium-binding proteins characterized by a tissue- and differentiation-specific expression pattern. None of the many functions assumed from in vitro experiments had ever been confirmed in vivo for any S100 protein. Making use of targeted disruption of the *MRP14* gene we here define the first physiologically relevant phenotype of a S100 family member. We show that MRP8 and MRP14 are essential for regulation of phagocyte migration. MRP8/MRP14 complexes integrate signals from 2 different signal transduction pathways, namely, calcium and the p38 MAPK cascade (Figure 1), thereby controlling reorganization of the MT system. We demonstrate that MRP8/MRP14 complexes promote formation of MTs in an MT-associated proteinlike fashion.[34] Morphologic evidence indicates that MRP8/MRP14 mediates cross-linking of tubulin filaments (Figure 3), thereby decreasing the flexibility of the MT system. In contrast to MRP14, MRP8 directly binds to tubulin and promotes its polymerization (Figures 2-3). This observation indicates that MRP8 is the active component of the MRP8/MRP14 complex and that MRP14 predominantly functions as a regulatory subunit. This is supported by the observation that MRP8$^{-/-}$ mice exhibit a lethal phenotype, most likely due to a defect in cell migration during early embryonic development.[17] The regulatory activity of MRP14 apparently involves at least 2 distinct mechanisms: (1) MRP14 stabilizes MRP8 and prevents its early degradation, as shown by significantly lower amounts of MRP8 protein in granulocytes from MRP14$^{-/-}$ mice despite normal mRNA levels. This interference is supported by the fact that in vivo almost all MRP8 is complexed to MRP14.[21,22,35,36] Furthermore, MRP8/MRP14 complexes are more effective in promoting tubulin polymerization in vitro than MRP8 monomers (Figure 3). (2) Activation of the p38 MAPK pathway in phagocytes results in phosphorylation of MRP14, which then antagonizes MT formation and stabilization promoted by MRP8/MRP14 complexes (Figures 1 and 3). In this context it is noteworthy that MRP14 is the major phosphate acceptor in phagocytes representing about 50% of phosphorylated protein after activation of p38 in monocytes.[23]

Both p38 MAPK signaling cascades and calcium-dependent signal transduction pathways have previously been shown to be involved in the regulation of leukocyte movement through the endothelium.[3,13,37] Various proinflammatory mediators are capable of activating the p38 pathway, for example, cytokines, chemokines, and bacterial products.[37-40] In addition, cross-linking of adhesion receptors during leukocyte-endothelial cell interaction results in activation of p38- and calcium-dependent pathways.[3,37,41] Activation of p38, in turn, modulates cytoskeletal dynamics during adhesion by an unknown mechanism,[3,39] whereas inhibition of p38 blocks adherence and chemotaxis of neutrophils.[38] Accordingly, we observed that MRP14 phosphorylation induced by the p38 pathway is associated with increased transmigration rates of MRP14$^{+/+}$ phagocytes. The functional relevance of MRP14 phosphorylation by p38 for transmigration is shown by the fact that MRP14$^{-/-}$ granulocytes, in contrast to MRP14$^{+/+}$ cells, failed to respond with

increased transmigration rates after activation of the p38 pathway (Figure 5A). Interestingly, interleukin 8 (IL-8), a potent activator of p38, also fails to increase migratory properties of MRP14$^{-/-}$ granulocytes.[19]

Compared to the MT network the actin cytoskeleton, which is not quantitatively altered in MRP14$^{-/-}$ mice, is assumed to be mainly responsible for transmigration events. However, modulation of MT dynamic instability by MRP8/MRP14 complexes may be functionally linked to the actin network, because enhanced MT turnover activates Rac1, Cdc42, and RhoA, which in turn control actin dynamics.[42,43] In phagocytes, RhoA regulates cell contraction, whereas Rac1 and Cdc42 control the formation of lamellipodia and filopodia, Cdc42 especially in response to a chemoattractive gradient.[5,6,43,44] Activation of small GTPases is dysregulated in MRP14$^{-/-}$ mice. Absence of the MRP8/MRP14 complex is associated with a substantially decreased expression of Rac1 and Cdc42. This is not due to changes at the transcriptional level (data not shown). It rather refers to the fact that binding of Rac1 and Cdc42 to MTs, which is diminished in MRP14$^{-/-}$ cells, probably delays metabolic turnover. More important, however, is the fact that activation of Rac1 and Cdc42 via the p38 signaling pathway is almost absent in MRP14$^{-/-}$ granulocytes, which is reflected by insufficient migration in the transendothelial migration assay in vitro and in the wound healing model in vivo. MRP14$^{-/-}$ phagocytes do not have a general defect of migration but rather a disturbance of a specific intracellular signaling pathway because recruitment of granulocytes to, for example, experimental peritonitis, is not altered.[19] The combinations of stimuli responsible for these differences in distinct forms of inflammation are not identified so far.

The results presented here provide a novel regulatory mechanism of phagocyte transmigration involving control by both MAPK- and calcium-dependent signaling in a cooperative fashion. In resting phagocytes high amounts of MRP8/MRP14 complexes stabilize MTs. Complex formation of MRP14 with MRP8 prevents phosphorylation of MRP14 in the case of isolated activation of the p38 MAPK (signal 1 in Figure 6; also Figure 1). To allow phosphorylation, concomitant generation of an independent second signal is required; elevation of intracellular calcium levels (signal 2 in Figure 6) induces conformational changes of the MRP8/MRP14 complex that are a prerequisite for subsequent phosphorylation of MRP14 by p38. Phosphorylation of MRP14 antagonizes the stabilizing effect of MRP8/MRP14 on MTs, which subsequently induces migration via activation of Rac1 and Cdc42.[42,43] Thus, 2 major activation pathways converge on the phagocyte-specific target molecules MRP8 and MRP14, which are of central importance for control of the migratory capacities of these cells. These findings may explain why MRP14$^{-/-}$ granulocytes exhibit a migratory phenotype that is dependent on a combination of distinct extracellular stimuli and thus is restricted to distinct kinds of inflammatory reactions. Pharmacologic interference with MRP14 phosphorylation may thus represent an interesting approach to modulate distinct inflammatory properties of phagocytes. Due to the restricted expression pattern of MRP8/MRP14, adverse effects on other cell types should be minimized. Such a strategy may be useful in the management of inflammatory diseases where monocytes and granulocytes expressing MRP8 and MRP14 play a prominent role.[45-49] Pharmacologic p38 inhibitors have already been shown to exhibit potent anti-inflammatory properties in various experimental models of inflammation.[13,50] Our results indicate that inhibition of p38-mediated phosphorylation of MRP14 may be a major mechanism responsible for these anti-inflammatory effects on phagocytes.

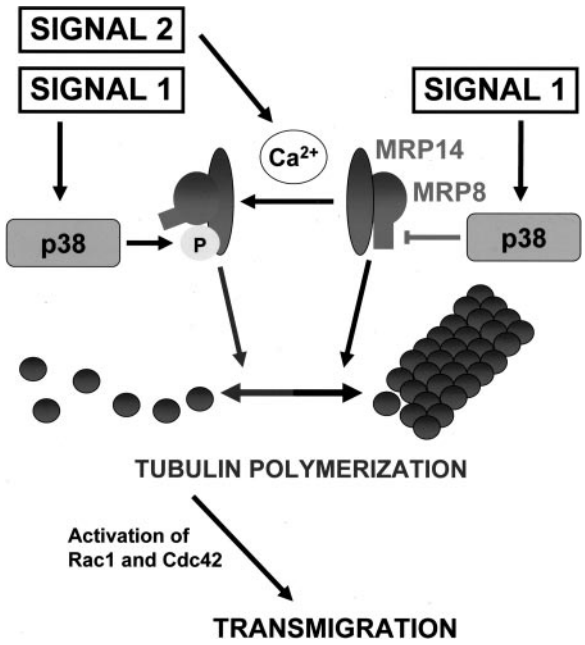

Figure 6. Role of MRP8 and MRP14 in cytoskeletal organization during transmigration of phagocytes. In resting phagocytes, MRP8/MRP14 complexes promote formation and stabilization of MTs. Isolated activation of the p38 MAPK signaling pathway (signal 1) has no effect because complex formation with MRP8 does not allow phosphorylation of MRP14. Concomitant calcium signaling (signal 2), however, induces conformational changes of the MRP8/MRP14 complex, which then permits phosphorylation of MRP14. The MT-stabilizing effect of MRP8/MRP14 complexes is thereby abrogated. After dissociation from depolymerizing MTs, small GTPases Rac1 and Cdc42 are activated and transmigration of granulocytes is facilitated.

Acknowledgments

We thank H. Hater, U. Keller, and G. Kiefermann for excellent technical assistance.

References

1. Springer TA. Traffic signals for lymphocyte recirculation and leukocyte emigration: the multistep paradigm. Cell. 1994;76:301-314.
2. Vestweber D. Molecular mechanisms that control endothelial cell contacts. J Pathol. 2000;190:281-291.
3. Pettit EJ, Fay FS. Cytosolic free calcium and the cytoskeleton in the control of leukocyte chemotaxis. Physiol Rev. 1998;78:949-967.
4. Sanchez-Madrid F, del Pozo MA. Leukocyte polarization in cell migration and immune interactions. EMBO J. 1999;18:501-511.
5. Jones GE. Cellular signaling in macrophage migration and chemotaxis. J Leukoc Biol. 2000;68:593-602.
6. Allen WE, Zicha D, Ridley AJ, Jones GE. A role for Cdc42 in macrophage chemotaxis. J Cell Biol. 1998;141:1147-1157.
7. Etienne-Manneville S, Hall A. Integrin-mediated activation of Cdc42 controls cell polarity in migrating astrocytes through PKC-zeta. Cell. 2001;106:489-498.
8. Hall A. Rho GTPases and the actin cytoskeleton. Science. 1998;279:509-514.
9. Rodriguez OC, Schaefer AW, Mandato CA, Forscher P, Bement WM, Waterman-Storer CM. Conserved microtubule-actin interactions in cell movement and morphogenesis. Nat Cell Biol. 2003;5:599-609.
10. Robinson JM, Vandre DD. Stimulus-dependent alterations in macrophage microtubules: increased tubulin polymerization and detyrosination. J Cell Sci. 1995;108:645-655.
11. Ding M, Robinson JM, Behrens BC, Vandre DD. The microtubule cytoskeleton in human phagocytic leukocytes is a highly dynamic structure. Eur J Cell Biol. 1995;66:234-245.
12. Davies EV, Hallett MB. Cytosolic Ca^{2+} signalling in inflammatory neutrophils: implications for rheumatoid arthritis (Review). Int J Mol Med. 1998;1:485-490.

13. Herlaar E, Brown Z. p38 MAPK signalling cascades in inflammatory disease. Mol Med Today. 1999;5:439-447.
14. Roth J, Vogl T, Sorg C, Sunderkotter C. Phagocyte-specific S100 proteins: a novel group of proinflammatory molecules. Trends Immunol. 2003;24:155-158.
15. Odink K, Cerletti N, Bruggen J, et al. Two calcium-binding proteins in infiltrate macrophages of rheumatoid arthritis. Nature. 1987;330:80-82.
16. Heizmann CW, Cox JA. New perspectives on S100 proteins: a multi-functional Ca^{2+}-, Zn^{2+}- and Cu^{2+}-binding protein family. Biometals. 1998; 11:383-397.
17. Passey RJ, Williams E, Lichanska AM, et al. A null mutation in the inflammation-associated S100 protein S100A8 causes early resorption of the mouse embryo. J Immunol. 1999;163:2209-2216.
18. Hobbs JA, May R, Tanousis K, et al. Myeloid cell function in MRP-14 (S100A9) null mice. Mol Cell Biol. 2003;23:2564-2576.
19. Manitz MP, Horst B, Seeliger S, et al. Loss of S100A9 (MRP14) results in a reduced IL-8 induced CD11b surface expression, a polarized microfilament system and a diminished responsiveness upon chemoattractants in vitro. Mol Cell Biol. 2003;23:1034-1043.
20. Rammes A, Roth J, Goebeler M, Klempt M, Hartmann M, Sorg C. Myeloid related protein (MRP) 8 and MRP14, calcium binding proteins of the S100 family, are secreted by activated monocytes via a novel, tubulin dependent pathway. J Biol Chem. 1997;272:9496-9502.
21. Roth J, Burwinkel F, van den Bos C, Goebeler M, Vollmer E, Sorg C. MRP8 and MRP14, S-100-like proteins associated with myeloid differentiation, are translocated to plasma membrane and intermediate filaments in a calcium-dependent manner. Blood. 1993;82:1875-1883.
22. Vogl T, Propper C, Hartmann M, et al. S100A12 is expressed exclusively by granulocytes and acts independently from MRP8 and MRP14. J Biol Chem. 1999;274:25291-25296.
23. van den Bos C, Roth J, Koch HG, Hartmann M, Sorg C. Phosphorylation of MRP14, an S100 protein expressed during monocytic differentiation, modulates Ca(2+)-dependent translocation from cytoplasm to membranes and cytoskeleton. J Immunol. 1996;156:1247-1254.
24. Edgeworth J, Freemont P, Hogg N. Ionomycin-regulated phosphorylation of the myeloid calcium-binding protein p14. Nature. 1989;342:189-192.
25. Strupat K, Rogniaux H, Van Dorsselaer A, Roth J, Vogl T. Calcium-induced noncovalently linked tetramers of MRP8 and MRP14 are confirmed by electrospray ionization-mass analysis. J Am Soc Mass Spectrom. 2000;11:780-788.
26. van den Bos C, Rammes A, Vogl T, et al. Copurification of P6, MRP8, and MRP14 from human granulocytes and separation of individual proteins. Protein Expr Purif. 1998;13:313-318.
27. Hunter MJ, Chazin WJ. High level expression and dimer characterization of the S100 EF-hand proteins, migration inhibitory factor-related proteins 8 and 14. J Biol Chem. 1998;273:12427-12435.
28. Seckler R, Wu GM, Timasheff SN. Interactions of tubulin with guanylyl-(beta-gamma-methylene) diphosphonate: formation and assembly of a stoichiometric complex. J Biol Chem. 1990;265: 7655-7661.
29. Keates RA. Effects of glycerol on microtubule polymerization kinetics. Biochem Biophys Res Commun. 1980;97:1163-1169.
30. Werner S, Smola H, Liao X, et al. The function of KGF in morphogenesis of epithelium and reepithelialization of wounds. Science. 1994;266:819-822.
31. Thorey IS, Roth J, Regenbogen J, et al. The Ca^{2+}-binding proteins S100A8 and S100A9 are encoded by novel injury-regulated genes. J Biol Chem. 2001;276:35818-35825.
32. Kielbassa K, Schmitz C, Gerke V. Disruption of endothelial microfilaments selectively reduces the transendothelial migration of monocytes. Exp Cell Res. 1998;243:129-141.
33. Weisenberg RC, Deery WJ. The mechanism of calcium-induced microtubule disassembly. Biochem Biophys Res Commun. 1981;102:924-931.
34. Walczak CE. Microtubule dynamics and tubulin interacting proteins. Curr Opin Cell Biol. 2000;12: 52-56.
35. Goebeler M, Roth J, Henseleit U, Sunderkötter C, Sorg C. Expression and complex assembly of calcium-binding proteins MRP8 and MRP14 during differentiation of murine myelomonocytic cells. J Leukoc Biol. 1993;53:11-18.
36. Vogl T, Roth J, Sorg C, Hillenkamp F, Strupat K. Calcium-induced noncovalently linked tetramers of MRP8 and MRP14 detected by ultraviolet matrix-assisted laser desorption/ionization mass spectrometry. J Am Soc Mass Spectrom. 1999; 10:1124-1130.
37. Rao KM. MAP kinase activation in macrophages. J Leukoc Biol. 2001;69:3-10.
38. Nick JA, Avdi NJ, Young SK, et al. Common and distinct intracellular signaling pathways in human neutrophils utilized by platelet activating factor and FMLP. J Clin Invest. 1997;99:975-986.
39. Nick JA, Avdi NJ, Young SK, et al. Selective activation and functional significance of p38alpha mitogen-activated protein kinase in lipopolysaccharide-stimulated neutrophils. J Clin Invest. 1999;103:851-858.
40. Krump E, Sanghera JS, Pelech SL, Furuya W, Grinstein S. Chemotactic peptide N-formyl-met-leu-phe activation of p38 mitogen-activated protein kinase (MAPK) and MAPK-activated protein kinase-2 in human neutrophils. J Biol Chem. 1997;272:937-944.
41. Schmidt A, Caron E, Hall A. Lipopolysaccharide-induced activation of beta2-integrin function in macrophages requires Irak kinase activity, p38 mitogen-activated protein kinase, and the Rap1 GTPase. Mol Cell Biol. 2001;21:438-448.
42. Goode BL, Drubin DG, Barnes G. Functional cooperation between the microtubule and actin cytoskeletons. Curr Opin Cell Biol. 2000;12:63-71.
43. Waterman-Storer CM, Salmon E. Positive feedback interactions between microtubule and actin dynamics during cell motility. Curr Opin Cell Biol. 1999;11:61-67.
44. Rogers SL, Gelfand VI. Membrane trafficking, organelle transport, and the cytoskeleton. Curr Opin Cell Biol. 2000;12:57-62.
45. Sampson B, Fagerhol MK, Sunderkotter C, et al. Hyperzincaemia and hypercalprotectinaemia: a new disorder of zinc metabolism. Lancet. 2002; 360:1742-1745.
46. Rugtveit J, Haraldsen G, Hogasen AK, Bakka A, Brandtzaeg P, Scott H. Respiratory burst of intestinal macrophages in inflammatory bowel disease is mainly caused by $CD14^+L1^+$ monocyte derived cells. Gut. 1995;37:367-373.
47. Frosch M, Strey A, Vogl T, et al. Myeloid-related proteins 8 and 14 are specifically secreted during interaction of phagocytes and activated endothelium and are useful markers for monitoring disease activity in pauciarticular-onset juvenile rheumatoid arthritis. Arthritis Rheum. 2000;43:628-637.
48. Frosch M, Vogl T, Seeliger S, et al. Expression of myeloid-related proteins 8 and 14 in systemic-onset juvenile rheumatoid arthritis. Arthritis Rheum. 2003;48:2622-2626.
49. Seeliger S, Vogl T, Engels IH, et al. Expression of calcium-binding proteins MRP8 and MRP14 in inflammatory muscle diseases. Am J Pathol. 2003;163:947-956.
50. Badger AM, Griswold DE, Kapadia R, et al. Disease-modifying activity of SB 242235, a selective inhibitor of p38 mitogen-activated protein kinase, in rat adjuvant-induced arthritis. Arthritis Rheum. 2000;43:175-183.